Computer Simulation of Hydrogen Thermodesorption

Yu. V. Zaika[*1], E. K. Kostikova[2]

[1,2]Institute of Applied Mathematical Research, Karelian Research Centre, Russian Academy of Sciences,
Pushkinskaya st. 11, Petrozavodsk, Russia 185910

[*1]zaika@krc.karelia.ru; [2]fedorova@krc.karelia.ru

***Abstract*-In the context of problems of hydrogen and thermonuclear power engineering intensive research is being conducted into ways to protect construction materials against hydrogen corrosion, chemical reactor design, materials suitable for hydrogen storage and transporting. Mathematical models help to specify physical-chemical ideas about the interaction of hydrogen and its isotopes with solids, to discover the limiting factors and to significantly reduce the expenses of experimental research by means of numerical simulation for different parameters and experimental conditions (including extreme ones). Classical diffusion models are often insufficient. The paper is devoted to the model and numerical solution of the boundary-value problems of hydrogen thermo desorption taking into account nonlinear sorption-desorption dynamics on the surface and its reversible capture in the bulk. Computational algorithms based on difference approximations and the results of computer simulation of the hydrogen thermo desorption flux from a structural material sample are presented.**

Keywords- Hydrogen Interaction with Solids; Surface Processes; Thermo Desorption Method; Nonlinear Dynamical Boundary-value Problems; Finite-difference Schemes; Computer Simulation

I. INTRODUCTION

Interest in the interaction of hydrogen with solids is a multi-faceted one [1-8]. It is sufficient to mention power-engineering, metals protection from hydrogen corrosion, chemical reactor design, rocket and missile engineering, vacuum engineering and technology problems. For instance, while tritium (radio hydrogen) will presumably be applied (in the long term) to thermonuclear reactors, the problem of tritium diffusion leakage and its accumulation in structural materials may arise. The main focus had been on the problem of hydrogen embrittlement of metals, but the focus of which is gradually shifting towards active use of hydrogen useful properties. Hydrides help to retain substantial amounts of this environmental-friendly energy source. Hence the high expectations attached to hydrogen batteries and motors (relatively safe: without high pressures or low temperatures). Another example: reversible metal alloyage by hydrogen is the basis for plastification and thermal hydrogen processing of titanium alloys. Some special topics are considered in [9-18]. Enthusiasts speak not only of hydrogen energy but also of hydrogen economy [4]. Mathematical models of hydrogen isotopes interaction with a solid and methods for their parametric identification are needed to enhance the performance of experimental research, solve applied problems and draw general conclusions. The focus will be on the problem of the hydrogen permeability of structural materials. Practice has shown that the limitations are not only diffusion processes inside the metal, but also physical-chemical effects on the surface [2, 3]. Furthermore, transfer parameters depend on the process characteristics of producing the material batch, and one needs effective measured curve processing algorithms instead of focusing on "tabular data". The physical-chemical properties of Me–H (metal-hydrogen) systems are highly varied. This paper does not suggest a universal hydrogen permeability model suitable for different applied problems. Leave aside the problems that can be formalized in terms of continuum mechanics, which is a separate wide-ranging topic. The goal is more modest. There is a need in the well-balanced model of hydrogen thermal desorption that takes into account the main transport processes in their dynamic interdependence. Adsorption, dissolution, diffusion, etc. per se are subjects for in-depth theoretical studies. Each additional coefficient however, leads to a leap to a new difficulty level of the inverse problem of parametric identification. The focus is on physical and chemical contents models, which correspond to real capacities of the experimental methods considered below. Only the direct problem of numerical simulation of hydrogen flux from structural material is considered.

II. HYDROGEN PERMEABILITY MODELS

A. Diffusion with Reversible Traps and (De)Sorption Models

Consider the hydrogen transfer through a test metal sample (plate thickness ℓ). Physical-chemical terminology will be used as little as possible. For brevity the metal membrane is considered, although it may be a multi alloy or intermetallic compound. Assume that heating is relatively slow, well nigh uniform, so that the temperature gradient is negligible, and the diffusion flow can be considered proportional to the concentration gradient. The concentration of dissolved hydrogen (monoatomic hydrogen) is low and partly it is compatible with traps. Here, traps are defined as the crystal structure micro defects that can capture hydrogen. Assume a system of differential equations as a model of diffusion with reversible capture

DOI: 10.5963/AMSA0303003

$$\partial_t c(t,x) = D(T)\partial_x^2 c(t,x) - a_1(T)c(t,x)[1 - z(t,x)z_{\max}^{-1}] + a_2(T)z(t,x), \quad (1)$$

$$\partial_t z(t,x) = a_1(T)c(t,x)[1 - z(t,x)z_{\max}^{-1}] - a_2(T)z(t,x), \quad (t,x) \in Q_{t_*}, \quad (2)$$

where t — time, $Q_{t_*} = (0,t_*) \times (0,\ell)$; $c(t,x)$ — diffusing hydrogen (monoatomic) concentration; $z(t,x)$ — captured diffusant concentration; D — diffusion coefficient; a_1, a_2 — coefficients of H atom capture by and escape from traps. The traps capacity is limited by $z_{\max}$. Concentration of diffusible hydrogen is relatively low. However, significant amounts of hydrogen can be accumulated into traps, so that the total quantity of hydrogen can be large. Values D, a_i are a function of current temperature $T(t)$ from Arrhenius's law, where D_0, a_{0i} are preexponential factors, and E_D, E_i — activation energies (R is the universal gas constant): $D = D_0 \exp\{-E_D/[R\,T(t)]\}$, $a_i = a_{0i} \exp\{-E_i/[R\,T(t)]\}$.

More disaggregate transfer models are known. Among other factors, one can take into account various diffusion channels (transcrystalline, grain boundary, along defects). In applied problems only limiting factors are highlighted in order to balance the model completeness with the feasibility of parametric identification by measured data. One should bear in mind that diffusion coefficient D data are systematized for different materials and temperatures in the reference book. Generally, however, these data are computed in the models where the diffusant concentration is believed to equal zero near the surface. However, if physical-chemical processes on the surface are taken into account (as it increasingly happens) D values should be interpreted as an initial approximation.

The main problems in computer simulation are associated with dynamic nonlinear boundary conditions. This is in agreement with measurement data indicative of a significant effect of surface processes [3]. Assume that the membrane surface is in contact with gaseous hydrogen. The boundary conditions are simulated (with allowance for adsorption and desorption processes) in the following manner:

$$c(0,x) = \bar{c}(x), z(0,x) = \bar{z}(x), \quad x \in [0,\ell], \quad (3)$$

$$c_0(t) = g(T)q_0(t), c_\ell(t) = g(T)q_\ell(t), \ t \in [0,t_*], \quad (4)$$

$$\frac{dq_0}{dt} = \mu s(T)p_0(t) - b(T)q_0^2(t) + D(T))\partial_x c(t,0), \quad (5)$$

$$\frac{dq_\ell}{dt} = \mu s(T)p_\ell(t) - b(T)q_\ell^2(t) - D(T)\partial_x c(t,\ell), \quad (6)$$

$$b(T) = b_0 \exp\{-E_b/[R\,T]\}, s(T) = s_0 \exp\{-E_s/[R\,T]\}.$$

Here $c_0(t) \equiv c(t,0)$, $c_\ell(t) \equiv c(t,\ell)$ — boundary bulk concentrations of diffusing monoatomic hydrogen; $q_0(t)$, $q_\ell(t)$ — concentration on the surface ($x = 0,\ell$); $g(T)$ — parameter of local equilibrium between concentration on the surface and in near-surface bulk; μ — kinetic coefficient; $s(T)$ — coefficient indicating that only a small amount of the "bombarding" hydrogen is caught as atoms on the surface (denote by s the adhesion coefficient, considering that this coefficient sums up the overall process balance of physisorption–dissociation–chemisorption of molecular gas into monoatomic form on the surface); $p_0(t)$, $p_\ell(t)$ — gaseous (H_2) pressures at relevant membrane side; $b(T)$ — desorption coefficient.

Formulas (4)–(6) are now clarified. Formula (4) mean that near-surface bulk concentrations $c_0(t)$, $c_\ell(t)$ proportionately follow current concentrations $q_0(t)$, $q_\ell(t)$ on the surface, and the dissolution rate is comparatively high. Consider flux balances (5), (6). Derivatives on the left-hand side of the expression denote hydrogen accumulation on the surface. The higher the external pressure of gaseous hydrogen, the more atoms per unit time fall on the surface unit area (first parts on the right side of the expressions). The second addends mean that part of the atoms hitting the surface reunite into molecule and escape from the surface (desorption flux). The last parts on the right side of expressions (5) and (6) correspond to the flux of hydrogen atoms toward or from the surface through diffusion in the bulk.

Hydrogen occurs in the model both as molecules and in monoatomic form. For consistency, the count is based on atoms: $[c] = 1/\text{cm}^3$, $[q] = 1/\text{cm}^2$, $[Dc_x] = [J] = 1/\text{cm}^2\text{s}$ ($J \equiv bq^2$). In the term of the kinetic theory of gases value μp determines the number of particles (H_2 molecules, in this context) hitting a unit area per unit time. Taking into account the dimensionless coefficient s, the additive component μsp will be further interpreted as the flux density of the atoms precipitated on the surface. This component is an integrated index with no partitioning of the process into stages. E exponents are named activation energies although they may represent linear combinations of activation energies and heat energies of unit steps of the processes and have different signs.

Remark 1: The model of rapid dissolution on the surface (4) is obtained from more general flux balance formulas

$$k^-(T)q_0(t) - k^+(T)c_0(t) = -D(T)c_x(t,0), \ k^-(T)q_\ell(t) - k^+(T)c_\ell(t) = D(T)c_x(t,\ell).$$

Coefficients k^-, k^+ characterize the rate of dissolution in the bulk and rise to the surface. If these processes in the given temperature range are essentially faster than diffusion ($Dc_x \approx 0$) one can get formula (4) where $g = k^-/k^+$. If the surface is isotropic (in terms of $E_{k^-} \approx E_{k^+}$), then $g(T)$ has weak dependence on temperature. Formally, it is possible to write the Arrhenius formula $g(T) = g_0 \exp\{-E_g/[RT]\}$, $E_g = E_{k^-} - E_{k^+}$, but the "activation energy" E_g is not necessarily positive.

DOI: 10.5963/AMSA0303003

Surface coverage and saturation in the bulk can be additionally taken into account:

$$k^-(T)\left[1-c_{0,\ell}(t)c_{\max}^{-1}\right]q_{0,\ell}(t)\ -k^+(T)[1-q_{0,\ell}(t)q_{\max}^{-1}]c_{0,\ell}(t)=\mp D(T)c_x|_{x=0,\ell}\,.$$

The presence of the "threshold" factor $(1-c/c_{\max})$ results in the following. If concentration c in the near-surface bulk is close to the maximum possible dissolution practically ceases. Value $\theta(t)=q(t)/q_{\max}$ signifies the degree of surface coverage. The adsorption flux density of H atoms (dissociative hydrogen chemisorbtion to the surface) can be simulated by formula $\mu s(T)p(t)(1-\theta(t))^2$ in balance Eqs. (5), (6). Within the low concentrations range the ratio $\theta\ll 1$ holds, which is in agreement with quadratic desorption, diffusion equation linearity and $D\neq D(c)$. Kinetic constant dependence on temperature ($\mu\sim 1/\sqrt{T}$) is usually ignored compared to exponent in $s(T)$.

Remark 2: It is not for all materials that the surface matters so much. Eqs. (4)-(6) should be replaced with the following boundary conditions of third kind for highly porous ("loose") materials:

$$\mu s(T)p_{0,\ell}(t)-b(T)c_{0,\ell}^2(t)=\mp D(T))\partial_x c|_{x=0,\ell}\,. \tag{7}$$

Formally, formula (7) is obtained from Eqs. (5), (6) at a low rate of accumulation ($\dot{q}\approx 0$) on the surface. The desorption coefficient is labeled with one letter although the values (including dimensions) are different in formulas (7) and (5), (6). Given the multistage process "average" coefficient b in condition (7) is an effective recombination coefficient [7].

B. Experimental Method

The thermal desorption spectrometry method (TDS) [1]. Gaseous hydrogen (under reasonably high pressurize $\bar{p}$) is fed into a chamber with a strip of the metal or alloy studied. The strip is heated by electric current to a preassigned, fixed temperature $\overline{T}$ to increase the sorption rate. After the sample had absorbed a sufficient amount of hydrogen (to the equilibrium saturated state), it is quenched (the heating current is turned off). The physical-chemical processes slow down sharply, and significant amounts of hydrogen stay inside the sample (in particular, in various trap). The chamber is then vacuumized and the sample is simultaneously reheated. The heating rule $T(t)$ $(t_0=0)$ can vary widely. Heating is usually linear $T(t)=T_0+vt$, from room temperature $T_0=T(0)$ to quite high temperature $T_{\max}$ (as long as degassing is discernible against the flux maximum background). Molecular hydrogen pressure in the chamber is measured by mass-spectrometer. The desorption flux from the surface controls the pressure. The desorption flux density is denoted by $J(t)$:

$$p(t)=\theta_1\int_0^t J(\tau)\exp\{(\tau-t)\theta_0^{-1}\}\,d\tau,\quad J(t)=b(t)q^2(t). \tag{8}$$

From now on the contracted notation will be used for simplification (identity sign is interpreted as equality by definition):

$$b(t)\equiv b(T(t)),g(t)\equiv g(T(t)),D(t)\equiv D(T(t)),a_i(t)\equiv a_i(T(t)),s(t)\equiv s(T(t)).$$

Symmetry conditions are fulfilled for the TDS method:

$$\begin{gathered}p(t)=p_0(t)=p_\ell(t),\quad q(t)=q_0(t)=q_\ell(t),\quad c_0(t)=c_\ell(t),\\ D(t)c_x(t,0)=-D(t)c_x(t,\ell),\bar{c}(x)=\bar{c}(\ell-x),\bar{z}(x)=\bar{z}(\ell-x).\end{gathered} \tag{9}$$

Constant θ_1 dependents on the strip surface area ($\theta_1=S\theta_2$). Values θ_0 and θ_2 are determined by the actual parameters of the experimental apparatus, such as chamber volume V and vacuum system evacuating capacity v ($\theta_0=V/v$).

Measurement model (8) was chosen relying on practical experience: hydrogen dose injection (delta pulse) into the chamber causes a surge in pressure with subsequent exponential decline. Eq. (8) is classical in the measurement theory. Specifics of the problem are reflected by function $J(t)$, in the differential notation $J(t)=(p(t)/\theta_0+\dot{p}(t))/\theta_1$.

After the preliminary equilibrium saturation had settled, then values $\bar{c},\bar{z}$

$$c(0,x)=\bar{c}=\text{const},\quad z(0,x)=\bar{z}=\text{const},\ x\in[0,\ell],$$

are a priori unknown at initial time moment ($t=0$), defined by reheating. But these values are related by

$$[1-\bar{z}z_{\max}^{-1}]a_1\bar{c}=a_2\bar{z}\ \text{ at }\ t=0\ (T=T(0))$$

due to diffusion equations with capture (1), (2). Moment t_* of the experiment completion is determined by $p(t)\approx 0, t\geq t_*,\ c(t_*,x)=z(t_*,x)=0,\ x\in[0,\ell]$. No matter how profound a vacuum is generated, some hydrogen will be retained in the sample even at very high t_* because of the pressure and interactions with traps. Thus, such equations should be interpreted asymptotically at anywhere. The relatively negligible amount of hydrogen is ignored.

Remark 3: Usually, the pressure derivative $\dot{p}(t)$ is neglected at slow heating: $J(t)=\eta p(t)=p(t)/(\theta_0\theta_1)$. The coefficient $\eta=1/(\theta_0\theta_1)$ is determined from calibration results. If the accuracy of η estimation is too low, one has to use relative unit measurements only (only the $J(t)/J_{\max}$ ratio is approximately known).

DOI: 10.5963/AMSA0303003

III. DIFFERENCE SCHEME FOR TDS-DEGASSING MODEL

Consider a symmetrical (in the terms of the experiment formulation) nonlinear equations system given a limited capacity of traps of different types:

$$\frac{\partial c}{\partial t} = D\frac{\partial^2 c}{\partial x^2} - \sum_{\nu=1}^{m}[a_\nu^-[1-Z_\nu]c(t,x) - a_\nu^+ z_\nu(t,x)],\ Z_\nu \equiv \frac{z_\nu(t,x)}{z_{\max}^\nu}, \tag{10}$$

$$\frac{\partial z_\nu}{\partial t} = a_\nu^-(T)[1-Z_\nu]c(t,x) - a_\nu^+(T)z_\nu(t,x),\ \ t\in(0,t_*),\ x\in(0,\ell), \tag{11}$$

$$c(0,x) = \varphi(x) = \varphi(\ell - x),\quad z_\nu(0,x) = \psi_\nu(x) = \psi_\nu(\ell - x), \tag{12}$$

$$\frac{dq}{dt} = \mu s(T)p(t) - J(t) \pm D(T)\frac{\partial c}{\partial x}\Big|_{0,\ell},\quad J(t) \equiv b(T)q^2(t), \tag{13}$$

$$c_0(t) = c_\ell(t) = g(T)q(t),\ \ t\in[0,t_*],\quad p(t) = \theta_1\int_0^t J(\tau)\exp\{[\tau - t]\theta_0^{-1}\}\,d\tau.$$

Here $z_\nu(t,x)$ is the concentration of hydrogen atoms trapped by defects of different types ($z_{\max}^\nu = \max z_\nu$); $a_\nu^{\mp}$ is coefficients of H trapping and escape. For practical purposes trapping is estimated in "integrated" form. If the defect is related not to microcavity, but, for example to hydride phase inclusions then $a_j^-(T) \equiv 0$, and $a_j^+(T)$ value is positive only after a critical temperature: $T(t) \geq T_{\text{crit}}$ had been reached. In this case the initial distribution $\psi_j(x)$ is assumed to be uniform. Diffusion, desorption and adhesion coefficients D, b, s depend on temperature T by the Arrhenius law; and the formula g, $a_\nu \approx \text{const}$ is expected in the $T\in[T^-,T^+]$ range. The heating is practically uniform and linear: $T(t) = T_0 + \nu t,\ \nu > 0$.

A. Initial Data Specification

The equilibrium concentration of saturation c̄ meets the formula $\mu s\bar{p} = b\bar{c}^2/g^2$ at $T = \overline{T}$ (derivatives in boundary condition (13) are equal to zero). The model corresponds to the range of $\bar{c} \propto \sqrt{\bar{p}}$ (Sievert's law). When the pressure is high, the surface saturation factor is taken into account in parameter s. With a short initial stage of TDS-experiment (cooling-down and vacuumization) there is a nearly uniform initial distribution $\varphi(x) = \overline{c}$. Constant $\psi_\nu(x) = \bar{z}_\nu$ for trap with reversible capture is determined from (11):

$$\partial_t = 0, T = \overline{T} \Rightarrow a_\nu^-(\overline{T})[1 - \bar{z}_\nu(z_{\max}^\nu)^{-1}]\bar{c} - a_\nu^+(\overline{T})\bar{z}_\nu = 0.$$

If considerable time had passed after saturation and before the onset of reheating ($t = 0$), it is reasonable to use $\varphi(x) = \bar{c} - A\,[x - \ell_0]^2$, $A > 0$, $2\ell_0 = \ell$ to specify the initial data. Constant A is determined by substituting $\varphi(x)$ into the "smooth start" condition $\dot{q}(0) = 0$ (the equality is conditional: start temperature T_0 and heating rate ν are sufficiently low). Function $\psi_\nu(x)$ is fixed by the formula

$$a_\nu^-(T_0)[1 - \psi_\nu/z_{\max}^\nu]\varphi - a_\nu^+(T_0)\psi_\nu = 0. \tag{14}$$

The problem initial data $\bar{z}_\nu \equiv \psi_\nu(x)$, T_{crit}, a_ν^+ for a hydride phase inclusion defect are derived from information about actual chemical compound of the hydride. Higher degrees are easy operated to formulate the initial distribution $c(0,x) = \varphi(x)$ without making essential changes.

The aim is to numerically model the desorption density $J(t) = b(t)q^2(t)$, $t\in[0,\ t_*]$ ($J(t) \approx 0$, $t \geq t_*$). This function is obtained experimentally, so that model flux $J(t)$ is needed for qualitative estimation to substantiate and test parametric identification methods. To wit information is needed on the effect of parameter (bulk and surface) variations on the dynamics of hydrogen thermal desorption from structural materials under non-stationary heating conditions.

B. Boundary-Value Problem: Difference Scheme

A grid $\bar{\omega}_h^\tau$ with steps τ, h on variables t, x in a closed region $\overline{\Omega} = [0,\ t_*]\times[0,\ \ell]$ is introduced. Denote by c_i^k approximate values of concentration $c(t_k,x_i)$; $z_{i,\nu}^k \approx z_\nu(t_k,x_i)$; $k\in\{0,\dots,M\}$, $i\in\{0,\dots,N\}$; $\tau = t_*/M$, $h = \ell/N$. Consider the scheme with weighting coefficients: $D = D(\xi_k)$, $a_\nu = a_\nu(\xi_k)$, $\xi_k\in[t_k,t_{k+1}]$,

$$\frac{c_i^{k+1} - c_i^k}{\tau} = (1-\sigma)[D\frac{c_{i+1}^k - 2c_i^k + c_{i-1}^k}{h^2} - \sum_{\nu=1}^{m}(a_\nu^-[1 - Z_{i,\nu}^k]c_i^k - a_\nu^+ z_{i,\nu}^k)]$$
$$+\sigma[D\frac{c_{i+1}^{k+1} - 2c_i^{k+1} + c_{i-1}^{k+1}}{h^2} - \sum_{\nu=1}^{m}(a_\nu^-[1 - \tilde{Z}_{i,\nu}^{k+1}]c_i^{k+1} - a_\nu^+ z_{i,\nu}^{k+1})],$$
$$\frac{z_{i,\nu}^{k+1} - z_{i,\nu}^k}{\tau} = (1-\sigma)[a_\nu^-[1 - Z_{i,\nu}^k]c_i^k - a_\nu^+ z_{i,\nu}^k] + \sigma[a_\nu^-[1 - \tilde{Z}_{i,\nu}^{k+1}]c_i^{k+1} - a_\nu^+ z_{i,\nu}^{k+1}].$$

DOI: 10.5963/AMSA0303003

Here, unknown value $Z_{i,\nu}^{k+1}$ is replaced (to realize the sweep algorithm on the $(k+1)$-th time layer) with its approximation from the finite-difference equation linear in $\tilde{Z}_{i,\nu}^{k+1}$

$$\tilde{Z}_{i,\nu}^{k+1} = Z_{i,\nu}^{k} + 0.5\tau[a_\nu^-(t_k)[1 - Z_{i,\nu}^k]c_i^k(z_{\max}^\nu)^{-1} - a_\nu^+(t_k)Z_{i,\nu}^k + a_\nu^-(t_{k+1})[1 - \tilde{Z}_{i,\nu}^{k+1}]c_i^k(z_{\max}^\nu)^{-1} - a_\nu^+(t_{k+1})\tilde{Z}_{i,\nu}^{k+1}]. \quad (15)$$

Standard nomenclature $\dot{y} = f(t,y)$ is used, this formula is an implicit scheme $y_{n+1} = y_n + 0.5\tau[f_n + f_{n+1}]$ for the differential Eq. (11) normalized to $z_{\max}^\nu$ with time-fixed function $c = c(t_k, x)$.The iterative procedure of specifying the values of $\tilde{Z}_{i,\nu}^{k+1}$ shall be described later.

Then assume $\sigma = 1/2$ and $\xi_k = t_k + \tau/2$. The approximation error is $O(\tau^2 + h^2)$. Denote $D(t_k + \tau/2) \equiv \hat{D}_k$ and $a_j(t_k + \tau/2) \equiv \hat{a}_{k,j}$, express $z_{i,\nu}^{k+1}$ from the second equation of the difference scheme and substitute it into the first equation. Using notations

$$V_i^k = \sum_{\nu=1}^{m} \frac{\hat{a}_{k,\nu}^-[1 - Z_{i,\nu}^k]}{\hat{a}_{k,\nu}^+ + 2\tau^{-1}}, \quad \tilde{V}_i^{k+1} = \sum_{\nu=1}^{m} \frac{\hat{a}_{k,\nu}^-[1 - \tilde{Z}_{i,\nu}^{k+1}]}{\hat{a}_{k,\nu}^+ + 2\tau^{-1}}, \; W_i^k = \sum_{\nu=1}^{m} \frac{\hat{a}_{k,\nu}^+ z_{i,\nu}^k}{\hat{a}_{k,\nu}^+ + 2\tau^{-1}}, \quad Q_i^{k+1} = 2 + \varkappa\hat{D}_k^{-1}(1 + \tilde{V}_i^{k+1}),$$

$$F_i^k = c_{i-1}^k - [2 - \varkappa\hat{D}_k^{-1}(1 - V_i^k)]c_i^k + c_{i+1}^k + 2\varkappa\hat{D}_k^{-1}W_i^k, \; \varkappa = 2h^2\tau^{-1},$$

the equations

$$c_{i-1}^{k+1} - Q_i^{k+1}c_i^{k+1} + c_{i+1}^{k+1} + F_i^k = 0 \;\; (k \geq 0) \quad (16)$$

are obtained.

Values at initial time moment $t = 0$ (on zero layer) are known: $c_i^0 = \varphi(x_i)$. Following the sweep method, approximate concentration values in grid-nodes on $(k+1)$-th time layer are searched for as follows

$$c_i^{k+1} = \alpha_i c_{i+1}^{k+1} + \beta_i + \gamma_i c_0^{k+1}, \quad i = 1,2,\dots,N-1, \quad k \geq 0. \quad (17)$$

The sweep coefficients are obtained by the formulas:

$$\alpha_i = [Q_i^{k+1} - \alpha_{i-1}]^{-1}, \; \beta_i = \alpha_i(\beta_{i-1} + F_i^k), \; \gamma_i = \gamma_{i-1}\alpha_i, \; i = 2,\dots,N-1.$$

Writing the ratio (16) for $i = 1$ initial coefficients $\alpha_1 = \gamma_1 = 1/Q_1^{k+1}$, $\beta_1 = F_1^k/Q_1^{k+1}$ are obtained.

The next task is to find the values c_0^{k+1}, c_N^{k+1} needed to run the sweep method. Substitute function $p(t)$ into boundary condition (13):

$$\frac{dq}{dt} = \mu s(T)\theta_1 \int_0^t J(\eta)\exp\{[\eta - t]\theta_0^{-1}\}\, d\eta - b(T)q^2(t) \pm D(T)\left.\frac{\partial c}{\partial x}\right|_{0,\ell}.$$

Write the difference approximation ($x = \ell$): $k \geq 0$, $p_k \equiv p(t_k)$, $D_k \equiv D(t_k)$,

$$\frac{q_{k+1} - q_k}{\tau} = 0.5[\mu s_k p_k - b_k q_k^2 - D_k\partial_x c(t_k, \ell) + \mu s_{k+1}p_{k+1} - b_{k+1}q_{k+1}^2 - D_{k+1}\partial_x c(t_{k+1}, \ell)]. \quad (18)$$

The integral is calculated approximately from the trapezoid formula:

$$p_{k+1} = \theta_1 \int_0^{t_{k+1}} J(\eta)\exp\{[\eta - t_{k+1}]\theta_0^{-1}\}d\eta = \exp\{-\tau\theta_0^{-1}\}p_k + \theta_1 \int_{t_k}^{t_{k+1}} \dots d\eta$$

$$\approx \exp\{-\tau\theta_0^{-1}\}p_k + 0.5\tau\theta_1[J_{k+1} + \exp\{-\tau\theta_0^{-1}\}J_k], \; p_0 = 0. \quad (19)$$

The second variant of p_{k+1} value calculation is the following. Apply the implicit scheme mentioned above for the equation $\dot{y} = f(t,y)$ to equation $\dot{p} = -p/\theta_0 + \theta_1 J$:

$$p_{k+1} = [(2\theta_0 - \tau)p_k + \theta_0\theta_1\tau(J_k + J_{k+1})][2\theta_0 + \tau]^{-1}.$$

Approximate in the boundary node with an accuracy up to $O(h^3)$

$$2h\partial_x c(t_j, \ell) \approx c_{N-2}^j - 4c_{N-1}^j + 3c_N^j, \quad j = k, k+1. \quad (20)$$

The values of concentration on the k-th time layer are known. Substituting values c_{N-2}^{k+1} and c_{N-1}^{k+1} from ratio (17) for the $(k+1)$-th time layer

$$\partial_x c(t_{k+1}, \ell) \approx \frac{1}{2h}[(3 + \alpha_{N-1}(\alpha_{N-2} - 4))c_N^{k+1} + (\gamma_{N-2} + \gamma_{N-1}(\alpha_{N-2} - 4))c_0^{k+1} + (\beta_{N-2} + \beta_{N-1}(\alpha_{N-2} - 4))].$$

DOI: 10.5963/AMSA0303003

Boundary concentrations are identical due to symmetrical initial data in the boundary value problem, therefore search for a solution of the problem such that $c_0^{k+1} = c_N^{k+1}$. Approximation of $\partial_x c(t_{k+1}, \ell)$ is written in a more compact form:

$$2h\partial_x c(t_{k+1}, \ell) \approx (H + G)c_N^{k+1} + B, \quad H \equiv 3 + \alpha_{N-1}\zeta, \tag{21}$$
$$G \equiv \gamma_{N-2} + \gamma_{N-1}\zeta, \qquad B \equiv \beta_{N-2} + \beta_{N-1}\zeta, \qquad \zeta \equiv \alpha_{N-2} - 4.$$

Formulas (19)–(21) are substituted into (18), denoting $c_N^{k+1} = y$:

$$[\frac{b_{k+1}}{g_{k+1}^2}(1 - \frac{\mu\theta_1\tau}{2}s_{k+1})]y^2 + [\frac{2}{\tau g_{k+1}} + \frac{D_{k+1}}{2h}(G + H)]y + \Gamma = 0,$$
$$\Gamma \equiv \frac{b_k}{g_k^2}(1 - \frac{\mu\theta_1\tau}{2}\exp\{-\tau\theta_0^{-1}\}s_{k+1})(c_N^k)^2 + \left(\frac{3D_k}{2h} - \frac{2}{\tau g_k}\right)c_N^k$$
$$+\frac{1}{2h}(D_{k+1}B + D_k(c_{N-2}^k - 4c_{N-1}^k)) - \mu p_k(\exp\{-\tau\theta_0^{-1}\}s_{k+1} + s_k).$$

For the second variant of determining pressure p_{k+1}

$$[\frac{b_{k+1}}{g_{k+1}^2}(1 - \frac{\mu\theta_0\theta_1\tau}{2\theta_0 + \tau}s_{k+1})]y^2 + [\frac{2}{\tau g_{k+1}} + \frac{D_{k+1}}{2h}(G + H)]y + \Gamma = 0,$$
$$\Gamma \equiv \frac{b_k}{g_k^2}(1 - \frac{\mu\theta_0\theta_1\tau}{2\theta_0 + \tau}s_{k+1})(c_N^k)^2 + (\frac{3D_k}{2h} - \frac{2}{\tau g_k})c_N^k$$
$$+ (2h)^{-1}(D_{k+1}B + D_k(c_{N-2}^k - 4c_{N-1}^k)) - \mu p_k(\frac{2\theta_0 - \tau}{2\theta_0 + \tau}s_{k+1} + s_k).$$

Physically, the positive root of the quadratic equation in y is chosen. The approximation accuracy of the boundary condition is $O(h^2 + \tau^2)$, which agrees with the difference scheme inside the bulk.

C. Computation Algorithm

Input values ℓ, D_0, E_D, b_0, E_b, s_0, E_s, g, $\bar{c} = \bar{c}(\bar{p}, \overline{T})$, T_0, v are known. For the parabolic simulation distribution $\varphi(x)$ $A > 0$ is found by substituting the distribution $\varphi(x) = \bar{c} - A[x - \ell_0]^2$ into the smooth start condition

$$\dot{q}(0) = 0: \quad A = \ell_0^{-2}[\bar{c} + \ell_0{}^{-1}Dg^2b^{-1}(1 - \sqrt{\bar{c}\ell bD^{-1}g^{-2} + 1})]|_{T_0}.$$

Set the type of defects, coefficients a_ν and calculate $\psi_\nu(x)$. The algorithm on the $(k+1)$-th layer $(k \geq 0)$ is the following.

1. Values $\tilde{Z}_{i,\nu}^{k+1}$ are calculated from Eq. (15) on the time layer.
2. Coefficient sets α, β, γ are iteratively computed by forward sweep stroke in accordance with formulas (16), (17).
3. Values in boundary nodes are determined by solving the quadratic equation in the variable $y = c_N^{k+1} = c_0^{k+1} > 0$.
4. Approximate values of concentration in all internal nodes of the grid are determined by backward sweep stroke by (17).
5. Pressure p_{k+1} and the values of concentration in defects (from the second equation of the difference scheme in the bulk) are computed using the formula

$$z_{i,\nu}^{k+1} = z_{i,\nu}^k + \frac{\hat{a}_{k,\nu}^-[(1 - Z_{i,\nu}^k)c_i^k + (1 - \tilde{Z}_{i,\nu}^{k+1})c_i^{k+1}] - 2\hat{a}_{k,\nu}^+ z_{i,\nu}^k}{\hat{a}_{k,\nu}^+ + 2\tau^{-1}}.$$

6. The correction of $\tilde{Z}_{i,\nu}^{k+1}$ values means that $\tilde{Z}_{i,\nu}^{k+1} = z_{i,\nu}^{k+1}/z_{max}^\nu$ can be assumed and the computations can be repeated as in sections until $\tilde{Z}_{i,\nu}^{k+1} \approx Z_{i,\nu}^{k+1}$ are stabilized (2–3 iterations are enough).

IV. COMPUTER SIMULATION RESULTS

Physical reasons and material balance are used as the calculation correctness indicator:

$$\int_0^\ell [\varphi + \sum \psi_\nu]dx + 2q(0) = \int_0^\ell [c(t,x) + \sum z_\nu(t,x)]dx + 2q(t) + 2\int_0^t J(\tau)\,d\tau.$$

Scaling was applied because of a wide range of magnitudes:

$$x = \ell\hat{x}, \hat{x} \in [0,1], \hat{c} = c/\bar{c} \in [0,1], \hat{z} = z/\bar{c}, \hat{q} = \hat{c}_{0,1}/(g\ell), \hat{D} = D/\ell^2, \hat{J} = \hat{b}\hat{q}^2, \hat{b} = b\bar{c}\ell, \hat{\mu} = \mu/(\bar{c}\ell).$$

DOI: 10.5963/AMSA0303003

Experimentally, ℓ value lies in the range $10^{-2} - 10^{-1}$ cm. Let concentration values be bounded by $\bar{c} \sim 10^{15} - 10^{19}\,\mathrm{cm}^{-3}$, $\bar{z} \sim 10^{14} - 10^{21}\,\mathrm{cm}^{-3}$. There are two types of traps (defects): with reversible capture and hydride phase inclusion. The examined limits of Arrhenius parameters are presented in Table 1.

TABLE 1 THE EXAMINED LIMITS OF ARRHENIUS PARAMETERS

Parameter	Range	Pre-exponential Factor	E, kJ/mol
D, cm^2/s	$10^{-10} - 10^{-4}$	$10^{-6} - 5 \cdot 10^{-2}$	$4 - 40$
b, cm^2/s	$10^{-26} - 10^{-17}$	$10^{-10} - 10^{-7}$	$35 - 100$
g, cm^{-1}	$1 - 10^4$	$1 - 10^4$	$-20 - 20$
a, $1/\mathrm{s}$	$10^{-6} - 10^{-2}$	$10^{-3} - 10^{-1}$	$0 - 20$

Data for tungsten are used in numerical experiments as the basic parameter set [7]:

$$\bar{c} = S(T)\sqrt{\bar{p}},\ \bar{p} = 670\,\mathrm{Torr}, \overline{T} = 1300\,\mathrm{K} \quad (\bar{c} = 5.08 \cdot 10^{16}\,\mathrm{cm}^{-3}),$$

$$S(T) = 2.113 \cdot 10^{18} \exp\{-100.344\,\mathrm{kJ}/[RT]\}\,\mathrm{cm}^{-3}\mathrm{Torr}^{-1/2},$$

$$b_{\mathrm{vol}}(T) = 6 \cdot 10^{-12} \exp\{-39.559\,\mathrm{kJ}/[RT]\}\,\mathrm{cm}^4\mathrm{s}^{-1},$$

$$D(T) = 4.1 \cdot 10^{-3} \exp\{-37.629\,\mathrm{kJ}/[RT]\}\,\mathrm{cm}^2\mathrm{s}^{-1}.$$

Here the coefficient $b = b_{\mathrm{vol}}$ is according to the model (7) with bulk desorption (effective recombination coefficient). Obtain $b = b_{\mathrm{surf}} = g^2 b_{\mathrm{vol}}$ for the considered model with surface desorption (13). Common parameter values for different curves in the figure are according to data for tungsten. In addition, The following basic values are set: $\ell = 10^{-1}$, $T_0 = 300$, $\dot{T} = 0.4$, $g_0 = 10^2$, $E_g = 0$, $b_0 = 6 \cdot 10^{-8}$, $\theta_0 = 20$, $\theta_1 = 2$, $a = 0$ (where traps are negligible).

In the model context, $\mu s\bar{p} = b_{\mathrm{vol}}\bar{c}^2$ for equilibrium state is obtained, which is in keeping with Sievert's law $\bar{c} = S\sqrt{\bar{p}}$. Here, $s(T) = b_{\mathrm{vol}}(T)S^2(T)/\mu$. To ensure definiteness in the numerical experiments relation $s(T)$ is fixed in consistency with b_{vol}, S data for tungsten and $\mu = 1.46 \cdot 10^{21}\,\mathrm{cm}^{-2}\mathrm{s}^{-1}\mathrm{Torr}^{-1}$. The values of $s(T)$ are within $10^{-12} - 10^{-4}$. Please note that $s(T)$ in the model is an integrated parameter and includes also the effect of the input surface coverage (for high pressures).

Equilibrium saturation $\bar{c}$ ($T = \bar{T}$) varied simultaneously with the model variation of b_{vol} (b_{surf} and g) since the external flux $\mu s\bar{p}$ is fixed. If the hydride phase (equispaced) formed the determined equilibrium concentration was considered to be the total (sum in the solution and the hydride phase). For reversible capture defects it is determined similarly. The initial (after cooling and vacuumization) distribution of dissolved hydrogen is fixed by parabolic distribution (but not including the dashed line curves in Figs. 1, 2). For reversible capture defects, the initial concentration $\psi(x)$ is computed in accordance with Eq. (14).

Varying coefficients are listed in the order of the maximums (from left to right or in descending order). Under heating TDS-degassing moves from the domain of control by surface processes to limitation by diffusion due to $E_b \gg E_D$. The wide range of dynamic "scanning" of the material is an essential advantage of the TDS-degassing method as opposed to the methods of permeability analysis at fixed temperatures. Contemporary vacuum units are strong enough to neglect resorption (return of a part of desorbed hydrogen to the surface) at the stage of degassing: $\mu sp = 0$. This statement has been validated numerically for the physically based range and the above parameters of θ_0, θ_1.

In paper [7] hydrogen permeability was analyzed at fixed temperature (constant pressure $p = \bar{p}$ was maintained on the input side, vacuum was created on the output side) for bulk desorption in accordance with (7) ($b = b_{\mathrm{vol}} = b_{\mathrm{surf}}/g^2$) and in the absence of defects. Thus stated, so called transport parameter $W = \ell b_{\mathrm{vol}} D^{-1} S\sqrt{\bar{p}}$ (where $S = \sqrt{\mu s/b_{\mathrm{vol}}}$ — was dissolution, $\bar{c} = S\sqrt{\bar{p}}$) was applied to the problem. This parameter appears through transition to dimensionless problem (add a substitution $\hat{t} = Dt/\ell^2$ to the above described normalizing). It was shown in the paper that keeping in mind experimental accuracy, surface processes were the limiting factor at $W < 10^{-2}$, and diffusion at $W > 10^4$. Let the focus be on this range of

$$W = b\ell D^{-1} g^{-1} \bar{q} \quad (\bar{c} = q\bar{q} = S\sqrt{\bar{p}}, S = g\sqrt{\mu s\bar{p}\, b^{-1}}, b = b_{\mathrm{surf}})$$

and for dynamic boundary conditions (5), (6), (13) at heating $T(t)$.

Numerical results are illustrated in Figs. 1-10. Fig. 1 shows that if one allows a significant amount of time before reheating ($c(0,x) = \bar{c} \to c(0,x) = \varphi(x) = \bar{c} - A[x - \ell_0]^2$), the flux reduction will be is more greater on the ascending part of the curves. The total amount of absorbed hydrogen will also be lower. There is the tendency for sticking together of initial ascending fronts (Fig. 2), which happens in practice, when diffusion is of essence alongside with surface processes. Please note that at a lower heating rate the image point of the plot migrated for a longer time and with a lower flux rate.

DOI: 10.5963/AMSA0303003

One can see in Fig. 3 that the pressure derivative ṗ and resorption can be neglected for a tungsten sample and at a heating rate v around tenth of K/s. An outburst of hydrogen emission from a hydride inclusion trap happened at $T = 800$ K. Since the TDS-spectrum has temperature on the abscissa, a "lower" curve ($v = 0.1$) corresponds to a longer duration experiment. The material balance is retained when calculating "on the t axis" (compare with Figs. 1, 2).

Curves with lines of higher intensity in Figs. 4, 5 correspond to tungsten parameters. The outward desorption flux increases with a reduction in pre-exponential factor b_0 and a rise of activation energy E_b. This pattern is due to the increase in equilibrium saturation concentration c̄ because of $\mu s\bar{p} = b_{\text{vol}}\bar{c}^2$ ($T = \overline{T}$). The same is true for g_0 effect (see also below Fig. 8, $b_{\text{vol}} = b_{\text{surf}}/g^2$). Fig. 5 illustrates a two peak structure emergence with an increase in E_b. In experimental studies emergence of a new peak is usually associated with additional release of hydrogen from traps with a higher activation energy (compare with Fig. 3 and Fig. 10). However Fig. 5 ($a = 0$) clearly shows that this effect may arise from the interplay of diffusion and desorption activation energies alone. At first desorption quickly "strips off" subsurface hydrogen resulting in the first splash. Decrease of $c_{0,\ell}$ results in a decrease of desorption. It also causes a sharp gradient of concentration in the bulk, which triggers a growing pumping from the bulk through diffusion… The same effect is seen at variation of other model parameters (Fig. 6-10). Use the logarithmic temperature scale in Fig. 6, because parameter D_0 strongly influences the duration of degassing. Fig. 9 illustrates that for the fast dissolution coefficient g value $E_g = 0$ is a "point of inflexion" when the surface behavior is isotropic: $E_{k^-} \approx E_{k^+}$.

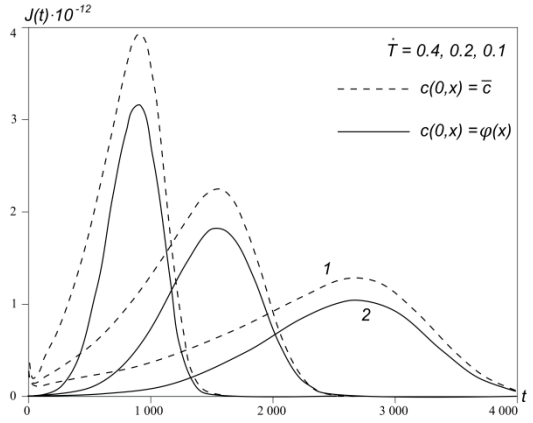

Fig. 1 Initial distribution: 1 – uniform, 2 – parabolic

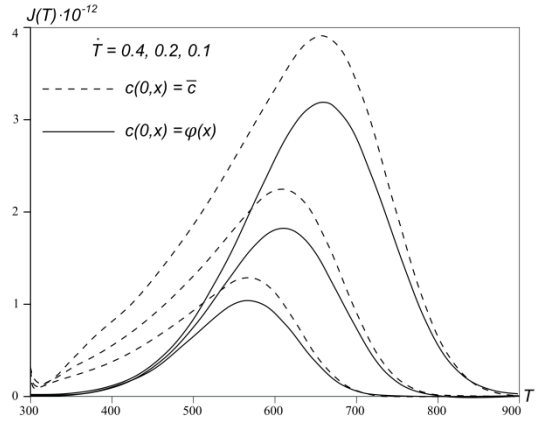

Fig. 2 Initial distribution: 1,2. TDS-spectrum

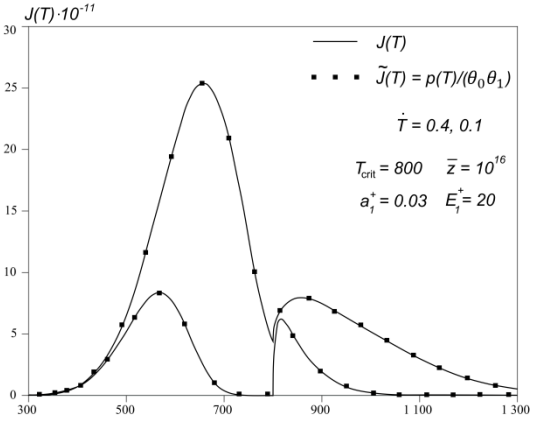

Fig. 3 Effect of hydride inclusion

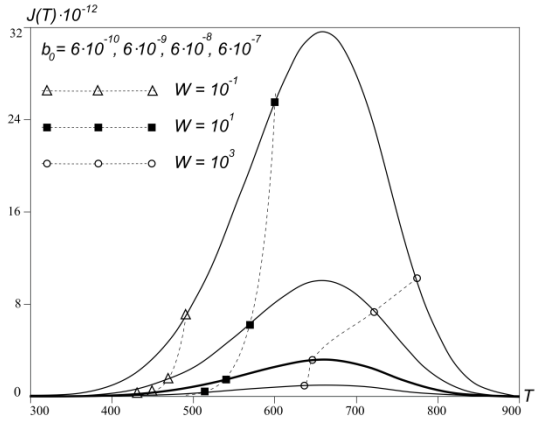

Fig. 4 Effect of parameter b_0

DOI: 10.5963/AMSA0303003

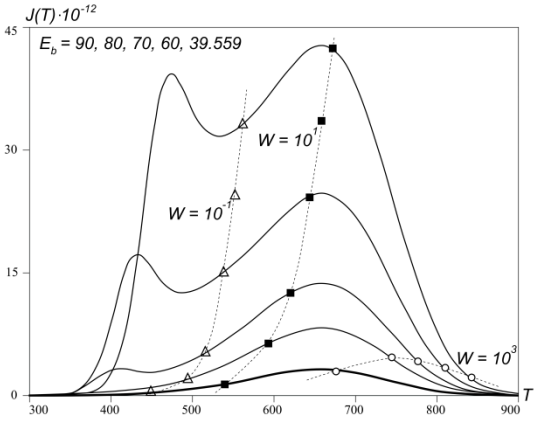

Fig. 5 Effect of parameter E_b

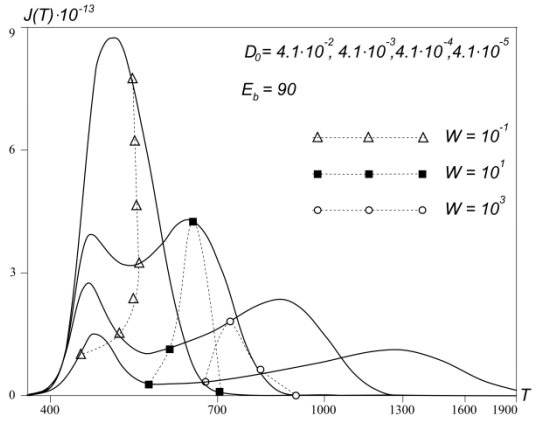

Fig. 6 Effect of parameter D_0

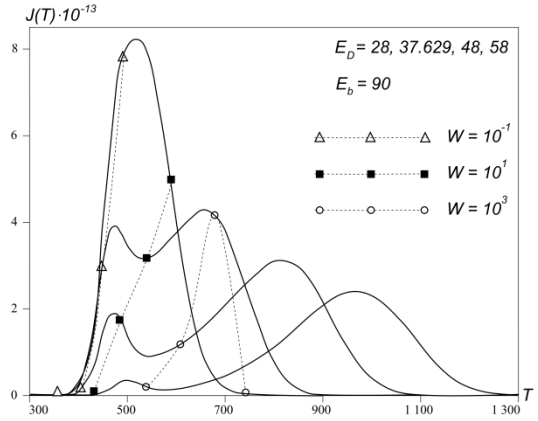

Fig. 7 Effect of parameter E_D

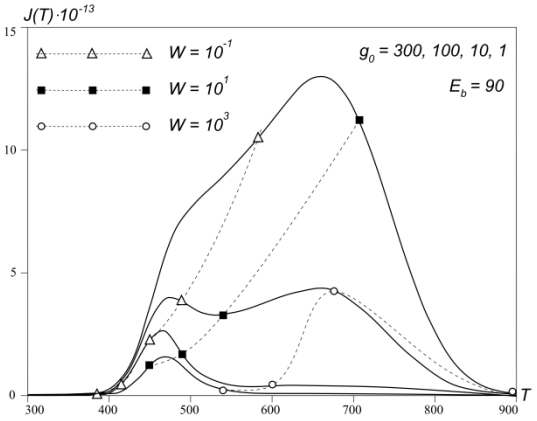

Fig. 8 Effect of parameter g_0

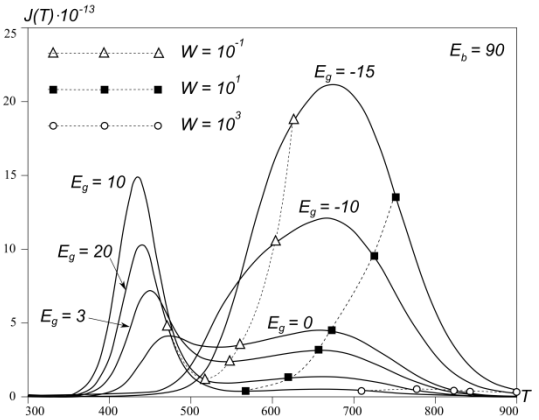

Fig. 9 Effect of parameter E_g

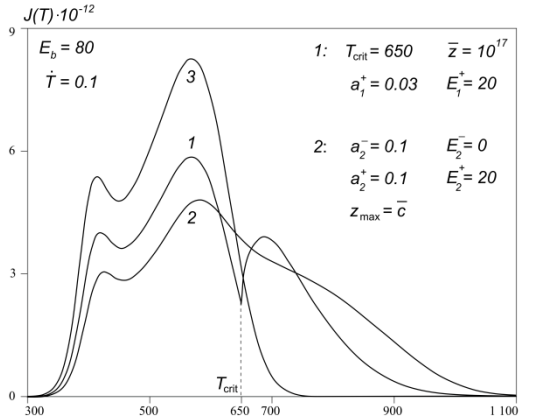

Fig. 10 Effect of defects: 1 – hydride inclusions; 2 – microcavities with reversible capture; 3 – without defects

V. CONCLUSIONS

The direct problem of computer simulation of the density of the thermal desorption hydrogen flux from a structural material sample was considered. A computational algorithm is proposed and realized. The TDS-method has advantages over the methods of hydrogen permeability at fixed temperature which consists in the feasibility of evolutional material scanning in

DOI: 10.5963/AMSA0303003

a wide range of temperatures (from limiting by surface processes to limiting by diffusion). Qualitative dependences of the flux and TDS-spectrum on experimental conditions are presented. Flux "derivatives" with respect to surface processes and diffusion parameters were estimated. It is shown that an extra peak is not always caused by traps with different hydrogen binding energies (as is commonly stated in the experimental works). This effect may be caused also by the difference between diffusion and desorption activation energies.

ACKNOWLEDGMENTS

The study was supported by the Basic Research Program of the Branch of Mathematics, Russian Academy of Sciences. Computer simulations were executed at the High-performance Data Treatment Centre in the Karelian Research Centre of RAS.

REFERENCES

[1] L. L. Kunin, A. M. Golovin, Yu. N. Surovoi, and V. M. Hohrin, *Problems of metals degassing*, Moscow: Nauka, 1972.

[2] G. Alefeld and J. Volkl, Eds., *Hydrogen in metals*, Berlin: Springer–Verlag, 1978.

[3] A. P. Zakharov, Ed., *Interactions of hydrogen with metals*, Moscow: Nauka, 1987.

[4] M. Ball and M. Wietschel, Eds., *The hydrogen economy*, Cambridge University Press, 2009.

[5] M. Hirscher, Ed., *Handbook of hydrogen storage: new materials for future energy storage*, Wiley–VCH, 2010.

[6] B. Sakintuna, F. Lamari-Darkrim, M. Hirscher, and B. Dogan, "Metal hydride materials for solid hydrogen storage: a review," *Int. J. of Hydrogen Energy*, Elsevier, vol. 32, no. 9, pp. 1121-1140, 2007.

[7] A. A. Pisarev, I. V. Tsvetkov, E. D. Marenkov, and S. S. Yarko, *Hydrogen permeability through metals*, Moscow: Nauka, 2008.

[8] R. A. Varin, T. Czujko, and Z. S. Wronski, *Nanomaterials for solid state hydrogen storage*, New York: Springer, 2009.

[9] F. J. Castro and G. Meyer, "Thermal desorption spectroscopy (TDS) method for hydrogen desorption characterization (I): theoretical aspects," *J. of Alloys and Compounds*, Elsevier, vol. 330-332, pp. 59-63, 2002.

[10] N. M. Vlasov and I. I. Fedik, "Hydrogen segregation in the area of threefold junctions of grain boundaries," *Int. J. of Hydrogen Energy*, Elsevier, vol. 27, pp. 921-926, 2002.

[11] D. A. Indeitsev and B. N. Semenov, "About a model of structure-phase transfomations under hydrogen influence," *Acta Mechanica*, vol. 195, pp. 295-304, 2008.

[12] B. Zajec, "Hydrogen permeation barrier—Recognition of defective barrier film from transient permeation rate," *Int. J. of Hydrogen Energy*, Elsevier, vol. 36, pp. 7353-7361, 2011.

[13] Yu. V. Zaika and N. I. Rodchenkova, "Modelling of diffusion TDS-spectrum peak of dehydriding with size reduction and heat absorption effects," *NATO Science for Peace and Security, Series C, Carbon Nanomaterials in Clean Energy Hydrogen Systems*, B. Baranowski, Ed., Springer, pp. 863-878, 2008.

[14] Yu. V. Zaika and N. I. Rodchenkova, "Boundary-value problem with moving bounds and dynamic boundary conditions: diffusion peak of TDS-spectrum of dehydriding," *Appl. Math. Modelling*, Elsevier, vol. 33, no. 10, pp. 3776-3791, 2009.

[15] N. I. Rodchenkova and Yu. V. Zaika, "Numerical modelling of hydrogen desorption from cylindrical surface," *Int. J. of Hydrogen Energy*, Elsevier, vol. 36, no. 1, pp. 1239-1247, 2011.

[16] Yu. V. Zaika and E. P. Bormatova, "Parametric identification of hydrogen permeability model by delay times and conjugate equations," *Int. J. of Hydrogen Energy*, Elsevier, vol. 36, no. 1, pp. 1295-1305, 2011.

[17] Yu. V. Zaika and N. I. Rodchenkova, "Hydrogen-solid boundary-value problems with dynamical conditions on surface," *Math. Modeling*, New York: Nova Sci. Publishers, pp. 269-302, 2012.

[18] Yu. V. Zaika and N. I. Rodchenkova, "Hydrogen-solid boundary-value problems with free phase transition interface," *Advances in Mathematics Research*, New York: Nova Sci. Publishers, vol. 15, pp. 128-180, 2012.

Yury V. Zaika was born in 1960, in USSR. Positions: Head of the Laboratory of Natural-Technical System Modelling, Institute of Applied Mathematical Research; Professor of Dept. of Applied Mathematics and Cybernetics, Petrozavodsk State University. Academic degrees: PhD (mathematical cybernetics), Leningrad (St. Petersburg) State University, 1985; Doctor (DSc) of Physics and Mathematics (mathematical modelling), St. Petersburg Institute for Informatics and Automation of RAS, 1998. Academic status: Professor (2002). Major research trends: Mathematical Theory of Control; Inverse Problems of Mathematical Physics; Mathematical Modelling of Hydrogen Interaction with Solids.

Ekaterina K. Kostikova was born in 1982, in Petrozavodsk, Russia. Positions: Researcher in the Laboratory of Natural-Technical System Modelling, Institute of Applied Mathematical Research (Petrozavodsk, Russia); Lecturer of Dept. of Applied Mathematics and Cybernetics, Petrozavodsk State University. Academic degree: Cand. (PhD) of Physics and Mathematics (2012, Petrozavodsk State University). Scientific specialty is mathematical modelling, numerical methods and software complexes. Major research trends: Mathematical Modelling of Physical Processes; Boundary-Value Problems of Mathematical Physics; Numerical Methods.

DOI: 10.5963/AMSA0303003